We are IntechOpen, the world's leading publisher of Open Access books
Built by scientists, for scientists

4,800
Open access books available

122,000
International authors and editors

135M
Downloads

154
Countries delivered to

Our authors are among the

TOP 1%
most cited scientists

12.2%
Contributors from top 500 universities

BOOK CITATION INDEX
CLARIVATE ANALYTICS
INDEXED

WEB OF SCIENCE™

Selection of our books indexed in the Book Citation Index
in Web of Science™ Core Collection (BKCI)

Interested in publishing with us?
Contact book.department@intechopen.com

Numbers displayed above are based on latest data collected.
For more information visit www.intechopen.com

Global Water Vapor Estimates from Measurements from Active GPS RO Sensors and Passive Infrared and Microwave Sounders

Shu-peng Ho and Liang Peng

Abstract

Water vapor plays an important role in both climate change processes and atmospheric chemistry and photochemistry. Global water vapor vertical profile can be derived from satellite infrared and microwave sounders. However, no single remote sensing technique is capable of completely fulfilling the needs for numerical weather prediction, chemistry, and climate studies in terms of vertical resolution, spatial and temporal coverage, and accuracy. In addition to the passive infrared and microwave sounder observations, the active global positioning system (GPS) radio occultation (RO) technique can also provide all-weather temperature and moisture profiles. In this chapter, we describe the current developments of global water vapor vertical profile and total precipitable water derived from active GPS RO measurements. In addition, we also demonstrate the potential improvement of global water vapor estimates using combined active GPS RO and passive IR/MW particularly from Atmospheric InfraRed Sounder (AIRS) and Advanced Technology Microwave Sounder (ATMS) measurements. Results show that because RO data are very sensitive to water vapor variation in the moisture rich troposphere, the RO data are able to provide extra water vapor information for the combined AIRS/ATMS and RO retrievals in the lower troposphere.

Keywords: water vapor, UT/LS, troposphere, greenhouse gas, climate process

1. Introduction

Water vapor is the major greenhouse gas in the atmosphere, which plays an important role in almost all the climate change processes. The transports and phase changes of water vapor directly affect the formation of cloud and precipitation, which modulate the hydrological cycle and the energy balance of the earth. Water vapor also has a strong effect on atmospheric chemistry and photochemistry. An accurate knowledge of the distribution of atmospheric water vapor is needed for climate change assessment, weather prediction, and atmospheric chemistry studies [1–3].

Global water vapor vertical profile can be derived from satellite infrared and microwave sounders (i.e., [4–8]). Nevertheless, no single remote sensing technique is able to completely fulfill the needs for numerical weather prediction, chemistry,

and climate studies in terms of vertical resolution, spatial and temporal coverage, and accuracy. Satellite infrared (IR) and microwave sounders have been routinely used for monitoring the temperature and moisture profiles in the mid and lower troposphere since 1980. Launched in 2002, Atmospheric InfraRed Sounder (AIRS) is a high spectral resolution radiometer onboard NASA Aqua satellite. With those more than 2000 high spectrum resolution channels in infrared wavebands, AIRS is able to provide excellent temperature and water vapor retrievals at the mid-troposphere level under clear skies. The AIRS measurements, together with more recent high spectrum resolution infrared (IR) measurements from Atmospheric Sounding Interferometer (IASI, 2006–current), and Cross-track Infrared Sounder (CrIS, 2011–current) have maintained continuous observations of tropospheric water vapor since 2002. However, due to the limitation of resolving power in terms of weighting functions and signal to noise ratio of these instruments, accurate estimates of water vapor concentration in the lower troposphere (LT) are still not available. Infrared sounders cannot sense atmospheric profiles below clouds.

While infrared data are limited to clear skies, microwave (MV) sounders can provide all sky data products. There are three main microwave radiometers with sufficient resolution and stability to measure tropospheric water vapor: the Advanced Microwave Sounding Unit-A (AMSU-A) and Advanced Microwave Sounding Unit-B (AMSU-B) on NOAA-15, 16, and 17 (i.e., N15, N16, and N17) satellites, the Microwave Humidity Sounder (MHS) on NOAA-18 (N18) and MetOp-A (Meteorological Operational satellite A) satellites, and Advanced Technology Microwave Sounder (ATMS) on Suomi National Polar orbiting Partnership (SNPP) and the first Joint Polar Satellite System (JPSS-1). These microwave sounders onboard the polar-orbiting satellites have been routinely used by NOAA to generate the tropospheric temperature and moisture profiles for all-sky conditions and hydrological variables (e.g., rainfall, precipitable water, cloud water, ice water, etc.) under cloudy conditions.

Using a one-dimensional variational (1DVAR) scheme, the NOAA Microwave Integrated Retrieval System (MiRS) inversion package is routinely applied to the AMSU/MHS sensors onboard the NOAA-18 (N18), NOAA-19 (N19), and Meteorological Operational Satellite-A (Metop-A) satellites to optimally retrieve temperature, moisture, and surface skin temperature (SST), as well as hydrometer variables within clouds over land and oceans [9, 10]. The MiRS-retrieved parameters have been validated globally using independent measurements [9, 11, 12]. However, studies demonstrated that the MiRS-derived hydrometer parameters within clouds over lands and oceans still contain uncertainty, especially in the lower troposphere [10]. This is partly because there is not enough information from the AMSU/ATMS measurements to completely resolve the hydrometer variables, temperature, and water vapor profiles under clouds.

In addition to the passive infrared and microwave sounder observations, the active global positioning system (GPS) radio occultation (RO) technique can also provide all-weather temperature and moisture profiles. Unlike passive MW and IR sensors, GPS RO is an active remote sensing technique that can provide all-weather, high vertical resolution (from ~100 m near the surface to ~1.5 km at 40 km) bending angle, and refractivity profiles [13, 14]. With knowledge of the precise positions and velocities of the GPS and low earth orbiting (LEO) satellites, which carry the GPS receivers, a vertical distribution of bending angles at the ray perigee point (the point of the ray path that is closest to Earth) can be derived. From the vertical distribution of the bending angle, we can derive a vertical distribution of the atmospheric bending angle and refractivity, which is a function of atmospheric temperature, moisture, and pressure [13, 14]. The GPS RO data have been intensively used for weather prediction and climate studies since the launch of the

FORMOSAT-3/COSMIC (Formosa Satellite Mission #3/Constellation Observing System for Meteorology, Ionosphere & Climate) satellite in 2006 [13, 15–22]. Different numerical methods and various assumptions for bending angle calculation can be found in [17, 22].

In this chapter, we describe the current developments of global water vapor vertical profile and total precipitable water derived from active GPS RO measurements. We will also demonstrate the potential improvement of global water vapor estimates using combined active GPS RO and passive IR/MW measurements. We introduce the COSMIC temperature and moisture products in Section 2. The combined inversion algorithm is summarized in Section 3. The inversion simulation results are summarized in Section 4. The validation of inversion results from the combined RO-AMSU retrievals using collocated radiosonde observation (RAOBs) is shown in Section 5. We conclude this study in Section 6.

2. COSMIC temperature and water vapor retrievals

COSMIC observations distribute relatively uniformly in space and time (see **Figure 1**). By placing a GPS receiver in LEO, GPS RO technique measures the phase delay of the radio signal from the GPS constellation precisely as the signal traverses the Earth's atmosphere. Being an active limb-sounding measurement, GPS RO technique is capable of retrieving profiles of microwave refractivity at very high vertical resolution [23]. The root mean square (RMS) error was estimated to be less than 1 K based on a detailed theoretical study [23], and this estimate was found to be consistent with numerous cross-validation studies between RO, radiosonde observation (RAOB), and other satellite measurements (e.g., [20, 21, 24–28]).

Although RO measurements are not sensitive to clouds, they are very sensitive to the vertical structure of atmospheric density profiles (a function of temperature, pressure, and water vapor profiles). When accurate RO observations, precise positions, and velocities of GPS and LEO satellites are known, accurate atmospheric temperature and moisture profiles can be derived [15, 29]. In a neutral atmosphere,
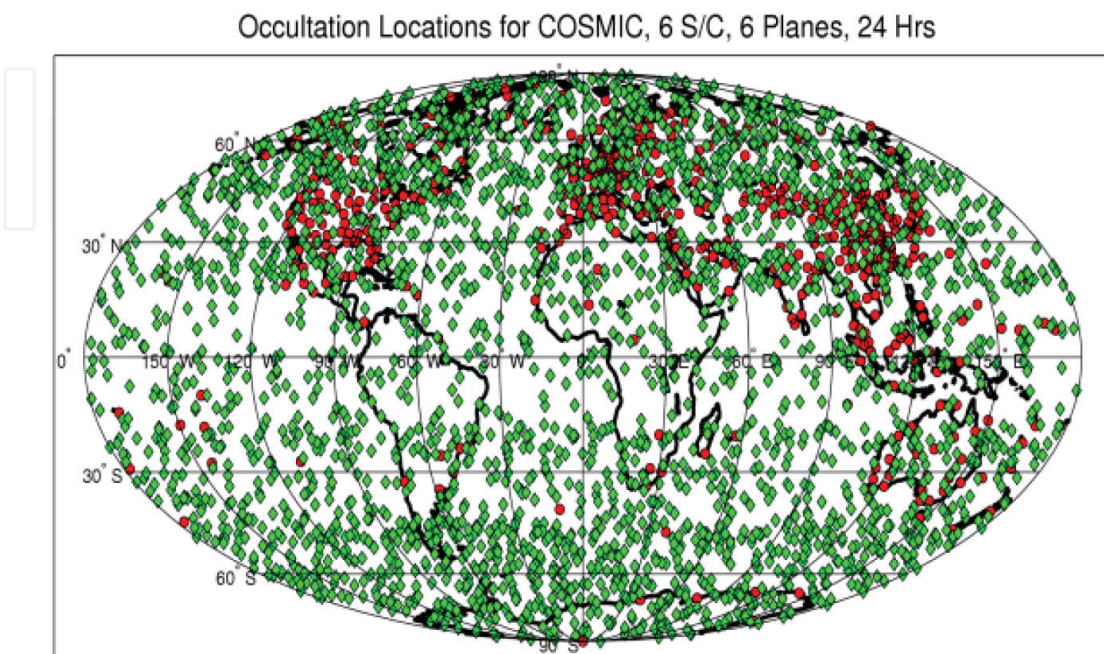

Figure 1.
Typical distribution of COSMIC GPS radio occultation soundings (green dots) over a 24-h period over the global. Red dots are the distribution of operational radiosonde stations.

the refractivity (N) is related to the pressure (P), the temperature (T), and the partial pressure of WV (PW) as represented by the following equation:

$$N = 77.6\frac{P}{T} + 3.73 \times 10^5 \frac{P_W}{T^2} \qquad (1)$$

Above the UT (∼8 km) where moisture is negligible, the dry temperature and the actual temperature are nearly equal [23]. The accuracy, precision, and long-term stability of RO data have been quantified by many studies under various atmospheric conditions [18–21, 26–28, 30]. GPS RO measurements have many important attributes that make them uniquely suitable for climate monitoring. These include: (i) no satellite-to-satellite bias, (ii) no instrument drift, and (iii) not affected by clouds and precipitation.

2.1 COSMIC temperature uncertainty

The distribution of water vapor profile depends on temperature [31, 32]. COS-MIC Data Analysis and Archive Center (CDAAC) is an international operational center that routinely inverses RO excess phase data obtained from multiple RO mission to bending angle and refractivity profiles. Recently, CDAAC has developed and installed new and improved RO inversion software, including improvements to precise orbit determination (POD), excess atmospheric phase computation, and neutral atmospheric inversion processing. Now these consistent RO inversion algorithms are applied to several international RO missions to derive the vertical distribution of bending angle, refractivity, temperature, and geo-potential height. These RO missions include GPS/MET (from 1995 to 1997, no overlap with other RO missions), COSMIC (launched in April 2006), Challenging Mini-satellite Payload (CHAMP, from 2001 to 2008), Gravity Recovery And Climate Experiment (GRACE, launched in 2004), Satélite de Aplicaciones Científicas-C (SAC-C, launched in 2000), GNSS RO Receiver for Atmospheric Sounding (GRAS, launched in 2007), Communication/Navigation Outage Forecast System (C/NOFS, launched in 2008), and Terra Synthetic Aperture Radar (SAR) operating in the X-band (TerraSAR-X, launched in 2007).

Currently, multi-year GPS RO climate data can be obtained from the GeoForschungsZentrum Potsdam (GFZ), Germany, the Jet Propulsion Laboratory (JPL), Pasadena, CA, USA, the University Corporation for Atmospheric Research (UCAR), Boulder, CO, USA, and the Wegener Center of the University of Graz (WegC), Graz, Austria. Different centers have used different assumptions, initializations, and implementations in the excess phase processing and inversion procedures, which may introduce refractivity differences between centers. Ho et al. [17] have used 5 years (2002–2006) of monthly mean climatologies (MMC) of retrieved refractivity from CHAMP generated by the above four centers to quantify the processing procedure-dependent errors. Results show that the absolute values of fractional refractivity anomalies among the centers are in general ≤0.2% from 8 to 25 km altitude (not shown). The median absolute deviation among the centers is less than 0.2% globally. This provides useful bounds on the errors introduced by data processing schemes.

The near real-time, postprocessing, and reprocessing status for all RO missions at CDAAC are summarized on the CDAAC website (http://cdaac-www.cosmic.ucar.edu/cdaac/products.html). A new version of Metop-A reprocessing, named Metop-A2016, has just finished processing and validation and will be posted to the CDAAC website in the next month. To illustrate the consistency between COSMIC

and Metop-A CDAAC products, **Figure 2** shows a statistical comparison for July 2014 of co-located COSMIC postprocessed (consistent with COSMIC2013) and Metop-A2016 reprocessed bending angle profiles. The match criteria used were: time differences <90 min and distances <250 km. The mean differences are very small. The differences in standard deviation at ∼30 km altitude (south pole region larger than north pole region) are believed to be due to stronger horizontal variability of the atmosphere during local winter. Remaining GPS RO missions will be processed as soon as possible, and all data will be made available via CDAAC's website.

RO derived temperature profiles especially in the lower stratosphere have also been intensively validated. **Figure 3** depicts that COSMIC temperature is very close to those from Vaisala-RS92 from 200 to 20 hPa (around 12 to 25 km). Note that, Vaisala-RS92 is one of the most accurate modern radiosondes where the structural uncertainties are ±0.2 K below 100 hPa and somewhat higher at higher levels. According to RS92 data continuity link under the Vaisala website, the Vaisala data including RS92 have been corrected for possible radiation errors. Their mean temperature difference in this height range is very close to zero. Because the quality of RO data does not vary with geophysical location and time, it is very useful to assess systematic errors of radiosonde sensors, whose characteristics may be affected by the changing environment and sensor types (e.g., [26, 28]). This result also shows the quality of RO temperature profiles where the precision of the mean of COSMIC-derived temperature profiles is estimated to be better than 0.05 K from 8 to 30 km [18].
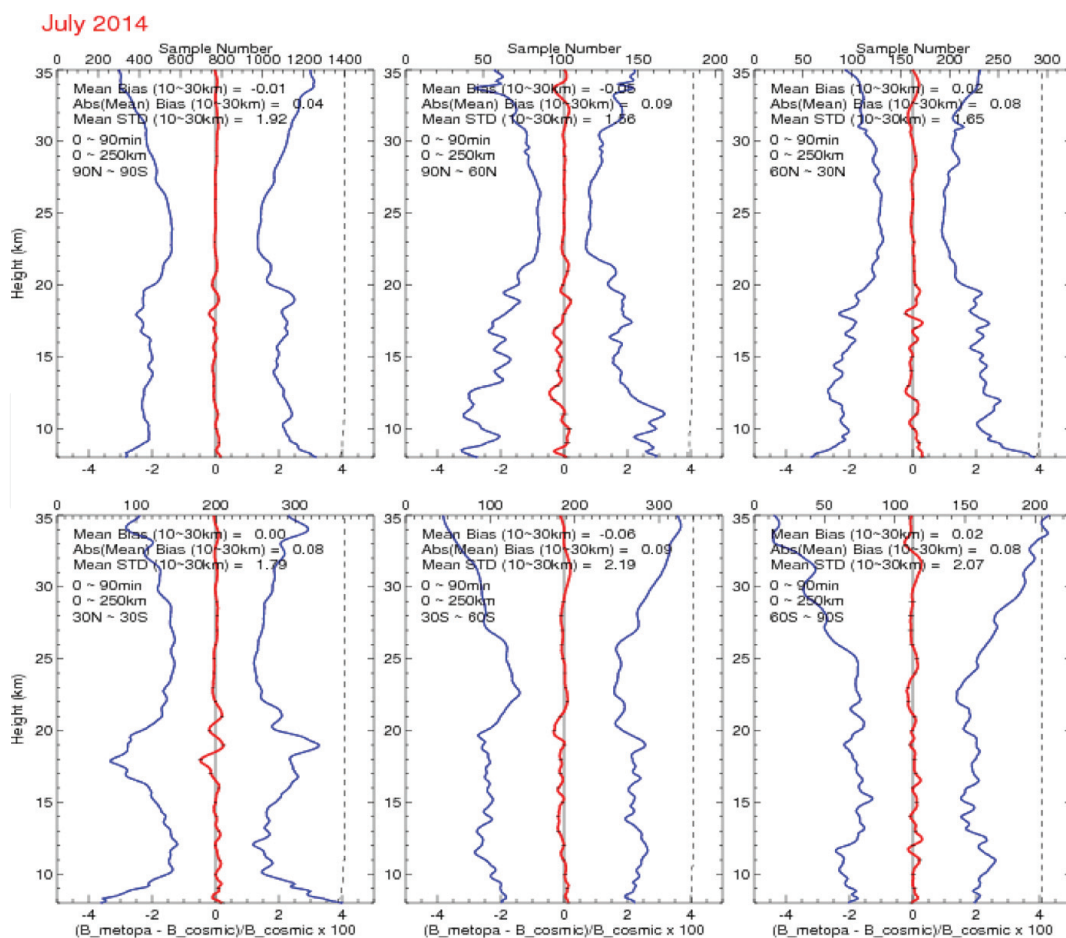

Figure 2.
Statistical comparison of co-located COSMIC postprocessed and Metop-A reprocessed bending angle profiles (red = mean and blue = standard deviation). Match criteria: time differences <90 min and distances <250 km.
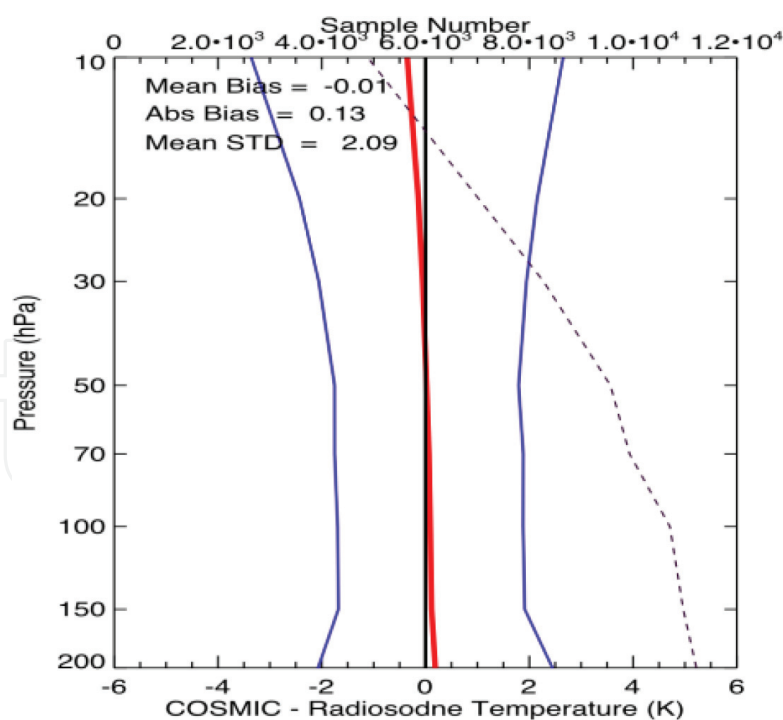
Figure 3.
Comparisons of temperature between COSMIC and radiosonde for Vaisala-RS92. Mean bias, absolute mean bias, and mean standard deviation from 200 to 10 hPa are computed. The red line is the mean difference, the blue line is the standard deviation, and the dotted line is the sample number. The top X axis shows the sample number.

2.2 COSMIC water vapor uncertainty

By using an advanced tracking technique, known as "open-loop tracking" [33], more than 90% of RO profiles from the COSMIC mission penetrate to below 2 km. As shown in Eq. (1), GPS RO refractivity is sensitive to temperature or water vapor, depending on the atmospheric conditions. Ho et al. [34] showed that in the upper troposphere where water vapor is negligible, RO observations are more sensitive to atmospheric temperature variations than to water vapor content. However, in the moisture rich troposphere, the RO refractivity is more sensitive to water vapor variation [34].

A 1D-var algorithm (http://cosmic-io.cosmic.ucar.edu/cdaac/doc/documents/1d var.pdf) is used to derive optimal temperature and water vapor profiles while temperatures and water vapor profiles from RO refractivity (see Eq. (1)). The ERA-Interim reanalyzes are used as a priori estimates for the 1D-var algorithm. The accuracy of COSMIC-derived total precipitation water (TPW) has been demon-strated by comparisons with TPW derived from ground-based GPS (i.e., Interna-tional Global Navigation Satellite Systems (IGS, [20, 35])) which are assumed not to be geolocation dependent. **Figure 4** (left panel) depicts COSMIC TPW and those from ground-based GPS collected within 2 h and 200 km in 2008. Only those COSMIC profiles whose lowest penetration heights are within 200 m of the height of ground-based GPS stations are included. Results demonstrate that the mean TPW difference between IGS and COSMIC is less than 0.2 mm with a standard deviation of 2.69 mm. This demonstrates the accuracy of COSMIC-derived water vapor in the lower troposphere, which should be particularly useful for improving AIRS/ATMS retrievals, especially over ice and cold surface backgrounds (see Sections 4 and 5). The right panel in **Figure 4** shows the time series of the COSMIC TPW and those from IGS at the same station. This demonstrates the importance and usefulness of COSMIC RO observations in depicting global water vapor variations.
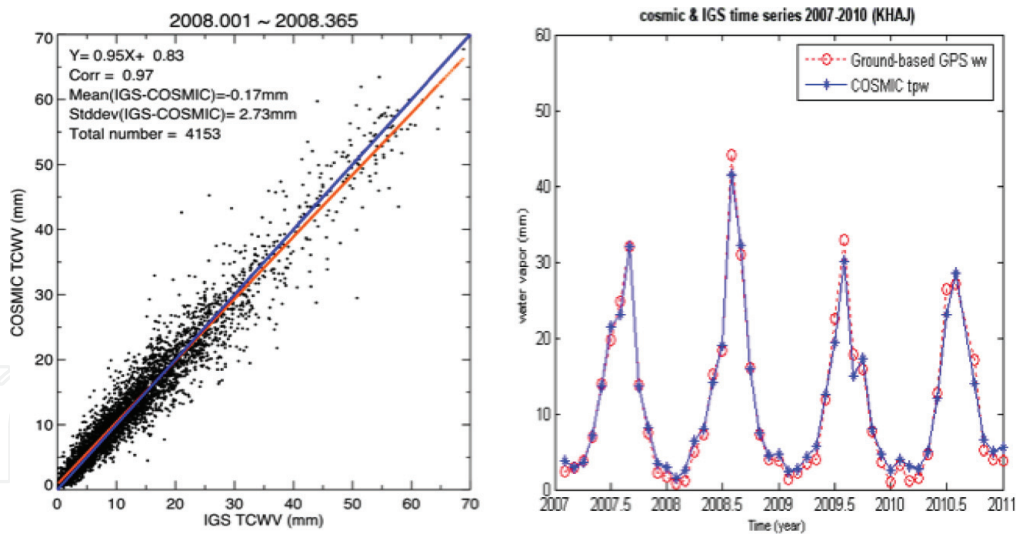
Figure 4.
Left panel: the global comparisons of total precipitable water (TPW) between COSMIC and those derived from ground-based GPS (i.e., IGS) for 2008. The right panel indicates the time series of IGS TPW and COSMIC-derived TPW near the IGS station.

COSMIC data have been used to study atmospheric temperature and refractivity trends in the lower stratosphere [17–19, 22] and variation of water vapor above, within, and below clouds [36–43]. COSMIC water vapor data have also been used to detect climate signals like El Niño-Southern Oscillation (ENSO; [38–40]), Madden-Julian Oscillation (MJO; [41]), atmospheric rivers [42, 43], and TPW variation owing to global warming [44–46].

In this study, we will use COSMIC data collocated with AIRS (COSMIC-AIRS pairs) and ATMS (COSMIC-ATMS pairs) to derive the temperature and moisture profiles. The relatively uniformly distributed COSMIC profiles in space and time would allow numerous RO and AIRS/ATMS coincident pairs, which would provide unprecedented atmospheric temperature and moisture profiles under various atmospheric conditions, which was not possible before.

3. The RO-ATMS and RO-AIRS inversion algorithms

3.1 RO-ATM inversion algorithm

As mentioned above, MiRS is a MW inversion package used by NOAA to perform a physical-based microwave retrieval in all-weather scenarios over all land-surface types. The MiRS data products have been routinely assessed using independent measurements [9, 11, 12]. The MiRS package can be downloaded, for free, at http://mirs.nesdis.noaa.gov/download.php. In this study, we revised the current MiRS algorithm and use measurements from ATMS collocate with RO data to develop an enhanced RO-ATMS inversion algorithm (i.e., RO-MiRS). We included the RO refractivity forward operator (Eq. (1)) into the RO-MiRS algorithm.

3.2 RO-AIRS inversion algorithm

Ref. [34] has detailed the information content for AIRS, RO, and the combined AIRS with RO for temperature and water vapor retrievals. Similar to the AIRS V6, the RO-AIRS inversion system is a 1D-var physical inversion system that retrieves the temperature and water vapor profiles sequentially. The updated fast and accurate AIRS transmittance model (Standard Alone AIRS-Radiance Transfer Algorithm

package—SARTA [47]) is served as an AIRS forward operator. The configurations of background covariance matrix, error covariance matrix, and *a priori* used in the concurrent RO-AIRS retrieval are detailed in [48] and are not further described here.

4. Simulation inversion of the combined measurements in the troposphere and lower stratosphere

4.1 Temperature and water vapor profiles derived from the combined RO-AIRS and RO-MW measurements in the troposphere and the boundary layer

To illustrate how the collocated RO data benefit the AIRS retrievals, we conduct a multiple variable regression simulation study to inverse RO and AIRS measurements simultaneously to obtain the temperature and water vapor profiles. The SARTA [47] is used to simulate the AIRS radiances. The simulated AIRS brightness temperatures (BTs) and RO refractivity measurements are computed by applying the NOAA-88b temperature and moisture profiles to AIRS and RO refractivity forward operators plus the known AIRS instrument noises and RO refractivity measurement noises, respectively.

The temperature and moisture root mean square errors (RMSEs) for RO, AIRS, and the combined RO and AIRS retrievals are plotted in **Figure 5**. It is demonstrated in **Figure 5** that the combined AIRS and RO observations act to constrain the individual solutions. The significantly improved water vapor RMSE is found in both the middle and lower troposphere. The RMSEs of water vapor mixing ratio for AIRS and RO improved from 1.5 and 1.0 g/kg at surface, respectively, to 0.5 g/kg for the GPS RO combined AIRS retrievals. Since GPS refractivity is less sensitive to temperature in the troposphere, only small temperature RMSE improvements are found.

The synergy of using RO observations with microwave observations has been demonstrated in numerous studies, including the comparison of Microwave Sounding Unit (MSU)/AMSU climate records with RO data in the upper troposphere [19], evaluating the accuracy of Special Sensor Microwave Imager (SSMI) water vapor retrievals [44–46, 49], and developing methods for concurrent
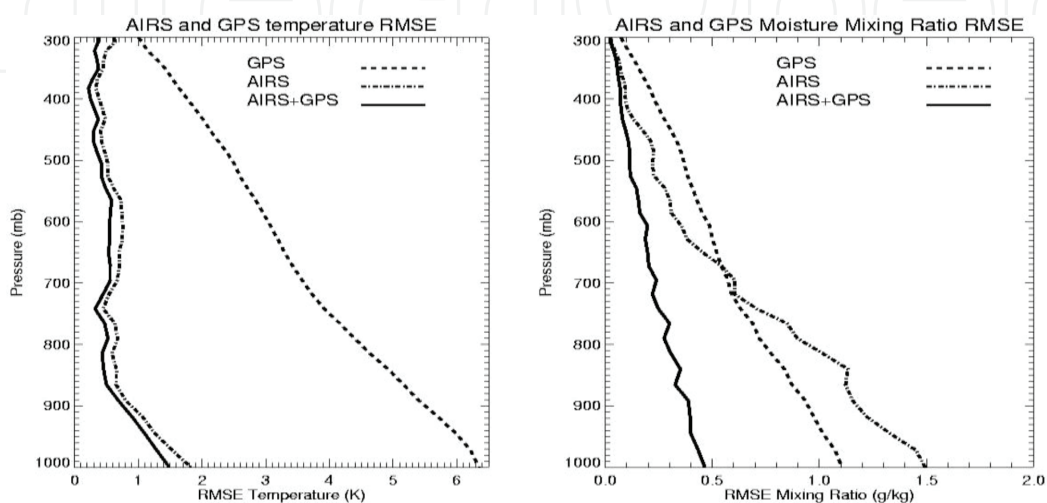
Figure 5.
The RMSE of retrieval results for temperature (left panel) and water vapor mixing ratio (right panel) for AIRS, GPS, and AIRS combined with GPS measurements.
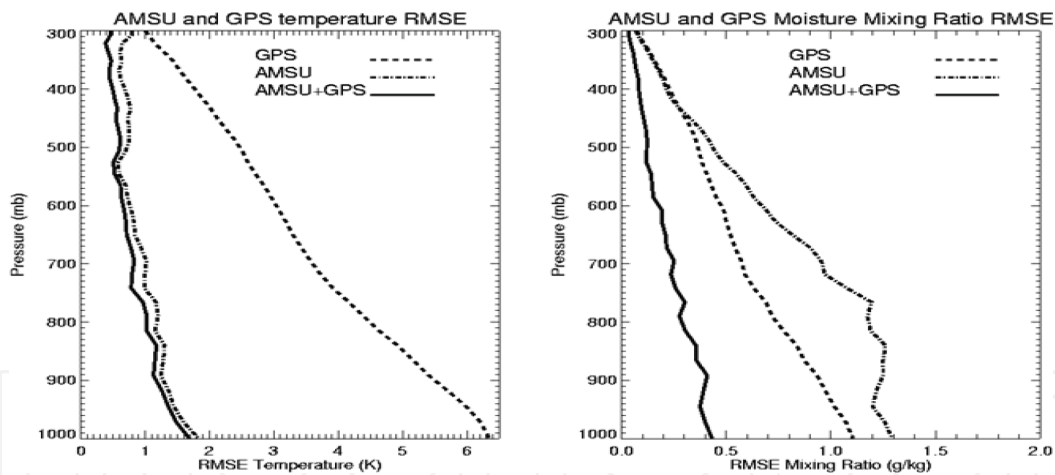
Figure 6.
The RMSE of retrieval results for temperature (left panel) and water vapor mixing ratio (right panel) for AMSU, GPS RO, and ASMU combined with GPS RO measurements over the globe.

inversion of RO and Atmospheric Infrared Sounder (AIRS) data [34, 48]. To illustrate how the increased amounts of RO data benefit the AMSU retrievals, we conduct a multiple variable regression simulation study using RO and MW measurements that are inversed simultaneously to retrieve the temperature and water vapor profiles. **Figure 6** shows the temperature and moisture RMSEs from the multiple variable regression simulation study of the GPS RO, AMSU, and the combined GPS RO and AMSU retrievals. The simulated AMSU BTs and RO refractivity measurements are computed by applying the NOAA-88b temperature and moisture profiles to AMSU and RO refractivity forward operators plus the known AMSU instrument noises and RO refractivity measurement noises, respectively.

It is shown in the right panel of **Figure 6** that because RO data are very sensitive to water vapor variation, the RMSEs for AMSU water vapor mixing ratio at the surface decreases from 1.3 g/kg (for AMSU only retrievals) to 0.4 g/kg when both GPS RO and AMSU data are used. The left panel of **Figure 6** shows that AMSU temperature measurements tremendously improve the GPS RO temperature retrieval when both GPS RO and AMSU data are used. These retrieval results demonstrate that the nadir viewing AMSU and limb-viewing GPS observations act to constrain the individual solutions; therefore providing much improved water vapor retrievals, particularly in the middle and lower troposphere. This is also demonstrated that by adding the RO refractivity operator in the AIRS inversion package described in [48], we are able to constrain the temperature and moisture profiles from the RO-AIRS observations and obtain the improved atmospheric thermal structure, which was not possible for individual sensors.

4.2 Improving the temperature and water vapor retrievals in the upper troposphere and stratosphere using combined AIRS, AMSU, and GPS RO measurements

In this section, we used GPS RO data to constrain the AIRS and AMSU temperature retrievals serving to improve moisture retrievals in the upper troposphere and lower stratosphere (UT/LS). In the upper troposphere, GPS RO refractivity is very sensitive to temperature but less sensitive to moisture. It is demonstrated by Ho et al. [34] that GPS RO refractivity can resolve temperatures greater than 1 K around 200 hPa but it can only sense about 15% of water vapor variation. **Figure 7** shows the temperature and moisture retrieval RMSE for AIRS, AMSU, and GPS RO as well as the combined AIRS, AMSU, and GPS RO data. The multi-variable
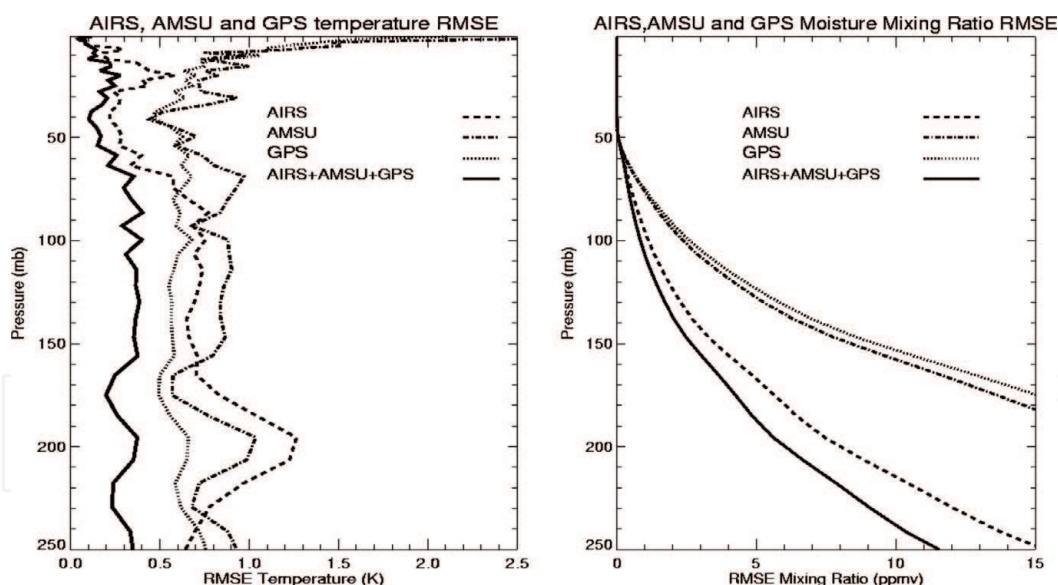
Figure 7.
The RMSE of temperature for AIRS, AMSU, GPS, and AIRS+AMSU+GPS in the UT/LS is on the left panel, and the RMSE of water vapor for AIRS, AMSU, GPS, and AIRS+AMSU+GPS in the UT/LS is on the right panel.

regression method described in Section 4.1 is used for the data from the simulation study. The 100 level AIRS vertical grids are used for all AIRS, AMSU, and GPS RO data. With a very high vertical resolution GPS RO refractivity profiles, AIRS and AMSU temperature RMSEs improved from 0.8 and 1.0 K, respectively, between 250 and 100 hPa (tropopause layer) to 0.4 K, which lead to AIRS and AMSU moisture RMSE around the same layer decrease from 4 and 15 ppmv, respectively, to around than 3 ppmv.

Since the open-loop tracking algorithm is only applied to COSMIC data, GPS RO data from COSMIC are used with AIRS data to derive moisture and temperature profiles in the clear skies of the free troposphere. For the UT/LS retrievals, GPS RO from SAC-C, GRACE, CHAMP, COSMIC, and GRAS data can be used to collocate with AIRS data. It can be seen in the left panel of **Figure 6** that the region of the largest temperature gradient is around 200 hPa, where the temperature RMSE for AIRS and AMSU is around 1.0 K. The fact that much improved temperature retrievals from GPS RO data (RMSE is ~0.6 K) and from the combined AIRS, AMSU, and GPS RO data (RMSE is ~0.3 K) are very useful to construct accurate temperature and moisture structures in the UT/LS region for the entire globe.

5. Initial results for the RO-MiRS retrievals from the COSMIC and ATMS data

We have successfully implemented the RO refractivity forward operator (Eq. (1)) into the current MiRS Version 11. This initial experiment is to demonstrate the feasibility of the proposed fusion approach to simultaneously retrieve global temperature and water profiles and hydrological data products using MiRS from the current operational COSMIC and ATMS data. Ten days of COSMIC-ATMS pairs are collected and inverted using RO-MiRS. **Figures 8** and **9** compared the co-located COSMIC and ATMS pairs (collected within 100 km and 15 min) with those temperature and moisture measurements from the Vaisala-RS92 radiosondes, respectively. **Figure 8** depicts that the mean temperature biases for RO/ATMS relative to
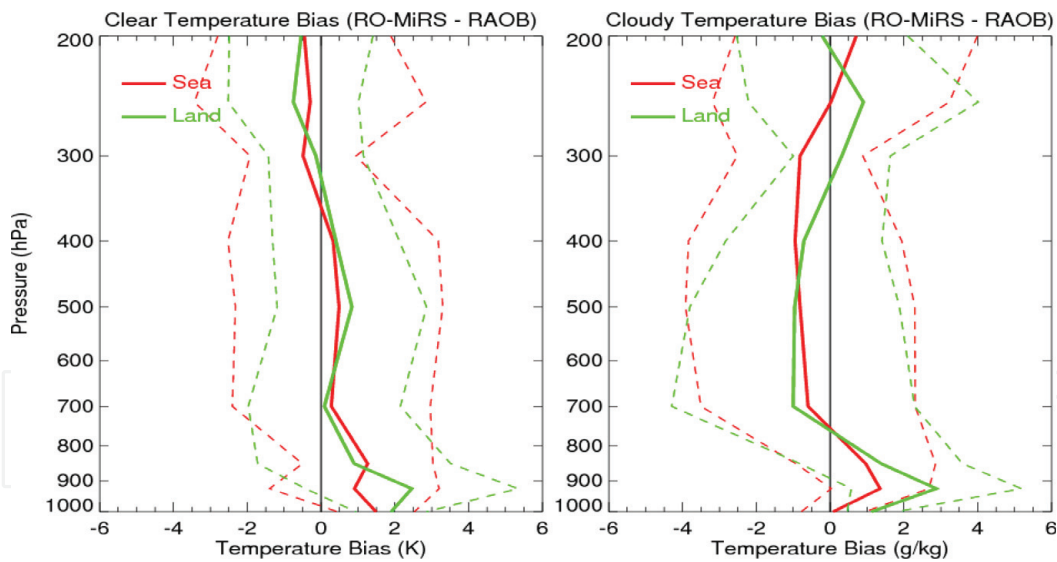
Figure 8.
RO-MiRS COSMIC/ATMS retrieved temperature bias with respect to co-located RS92 measurements (red: ocean and green: land) for clear (left) and rainy (right) conditions.
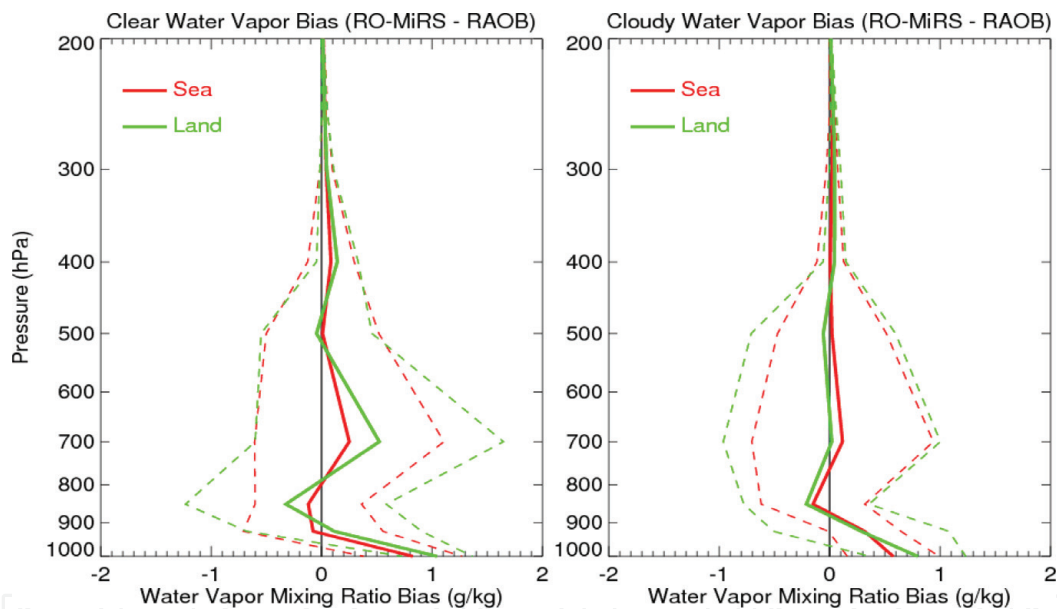

Figure 9.
RO-MiRS COSMIC/ATMS retrieved water vapor bias with respect to co-located RS92 measurements (red: ocean and green: land) for clear (left) and rainy (right) conditions.

those from RS92 are equal to 0.39 K with a standard deviation of 2.26 K for clear ocean cases and 0.0 K with a standard deviation of 2.35 K for cloudy ocean cases, respectively. The temperature biases for RO/ATMS results are larger from those over land than from those over oceans for both clear and cloudy conditions.

Figure 9 shows comparison results for RO/ATMS global water vapor retrievals. Over ocean surfaces, the retrieved bias is relatively low at all layers. The land retrievals show a larger bias than those over oceans. The global mean water vapor biases from surface to 200 mb for clear/sea, clear land, cloudy/sea, and cloudy/land cases are 0.11, 0.17, 0.11, and 0.11 g/kg, respectively. The temperature and water vapor biases for ATMS-only retrievals relative to those from RS92 are about 10–20% larger than the COSMIC/ATMS results at different levels (not shown).

6. Conclusions

In this study, we summarized research studies for quantifying global water vapor variation estimated using measurements from active GPS RO sensors and passive infrared and microwave sounders. A new inversion algorithm by inverting the GPS RO observations collocated with the NASA Aqua AIRS measurements to retrieve enhanced temperature and water vapor profiles is introduced. This effort is meant to generate improved temperature and moisture profiles, which are not possible by each individual sensors at the locations and times for the RO-AIRS collocated pairs. In addition, we also introduce a new approach for retrieving RO data with collocated MW measurements. By including the RO refractivity forward operator into the currently available MiRS package, we are able to provide the improved temperature and moisture profile in the troposphere.

In the combined RO and AIRS retrieval (for simulation experiments), the high vertical resolution RO retrieved temperature profiles are able to help to resolve the sharp temperature inversion layer in the UT/LS (i.e., the tropopause) and constrain AIRS water vapor retrieval in the same altitude. Because RO data are also very sensitive to water vapor variation in the moisture rich troposphere, the RO data shall also help to provide extra water vapor information for the combined AIRS and RO retrievals in the lower troposphere. It is demonstrated that the combined AIRS and RO observations act to constrain the individual solutions, the significantly improved water vapor RMSE is found in both the middle and lower troposphere. The RMSEs of water vapor mixing ratio for AIRS and GPS RO improved from 1.5 and 1.0 g/kg at surface, respectively, to 0.5 g/kg for the GPS RO combined AIRS retrievals. Since GPS refractivity is less sensitive to temperature in the troposphere, only small temperature RMSE improvements are found. Similar results are found in the COSMIC, ATMS, and ATMS+COSMIC retrieval results.

In future, we will apply AIRS and COSMIC data from 2006 to 2016 to the derived physical inversion algorithm and validate the retrieval results against in situ data. COSMIC's success has also prompted U.S. agencies to move forward with a follow-on FORMOSAT-7/COSMIC-2 (hereafter COSMIC-2) RO mission with Taiwan. The mission will launch six satellites into low-inclination orbits in early 2018 which is expected to yield up to 6000 uniformly distributed RO profiles per day. This would allow numerous RO and AMSU/ATMS coincident pairs after 2018, which would provide unprecedented atmospheric thermal and hydrometer information below clouds under various atmospheric conditions, which was not possible before.

Author details

Shu-peng Ho* and Liang Peng
COSMIC Project Office, University Corporation for Atmospheric Research, Boulder, Colorado, USA

*Address all correspondence to: spho@ucar.edu

IntechOpen

References

[1] Hartmann DL. Climate change, tropical surprises. Science. 2002;**295**: 811-812

[2] Crook NA. Sensitivity of moist convection forced by boundary layer processes to low-level thermodynamic fields. Monthly Weather Review. 1996; **124**:1767-1785

[3] Mason BJ. Recent improvements in numerical weather prediction. GARP Publication Series 26. 1986;**II**: 295-311

[4] Wentz FJ, Spencer RW. SSM/I rain retrievals within a unified all-weather ocean algorithm. Journal of the Atmospheric Sciences. 1998;**56**: 1613-1627

[5] Fetzer EJ, Lambrigtsen BH, Eldering A, Aumann HH, Chahine MT. Biases in total precipitable water vapor climatologies from atmospheric infrared sounder and advanced microwave scanning radiometer. Journal of Geophysical Research. 2006;**111**: D09S16. DOI: 10.1029/2005JD006598

[6] John VO, Soden BJ. Temperature and humidity biases in global climate models and their impacts on climate feedbacks. Geophysical Research Letters. 2007;**34**:L18605. DOI: 10.1029/ 2007GL030736

[7] Fetzer EJ, Read WG, Waliser D, Kahn BH, Tian B, Vömel H, et al. Comparison of upper tropospheric water vapor observations from the microwave limb sounder and atmospheric infrared sounder. Journal of Geophysical Research. 2008;**113** (D22):D22110

[8] Noël S, Buchwitz M, Burrows JP. First retrieval of global water vapour column amounts from SCIAMACHY measurements. Atmospheric Chemistry and Physics. 2004;**4**:111-125

[9] Boukabara S-A, Garrett K, Chen W, Liu Q, Yan B, Weng F. Global coverage of total precipitable water using a microwave variational algorithm. IEEE Transactions on Geoscience and Remote Sensing. 2010;**48**(10):3608-3621

[10] Boukabara S-A, Garrett K, Chen W, Iturbide-Sanchez F, Grassotti C, Kongoli C, et al. MiRS: An all-weather 1DVAR satellite data assimilation & retrieval system. IEEE Transactions on Geoscience and Remote Sensing. 2011; **49**(9):3249-3272. DOI: 10.1109/ TGRS.2011.2158438

[11] Iturbide-Sanchez F, Boukabara S-A, Chen R, Garrett K, Grassotti C, Chen W, et al. Assessment of a variational inversion system for rainfall rate over land and water surfaces. IEEE Transactions on Geoscience and Remote Sensing. 2011;**49**(9):3311-3333. DOI: 10.1109/TGRS.2011.2119375

[12] Kongoli C, Boukabara S-A, Yan B, Weng F, Ferraro R. A new sea-ice concentration algorithm based on microwave surface emissivities. IEEE Transactions on Geoscience and Remote Sensing. 2011;**49**(1):175-189

[13] Anthes RA, Bernhardt PA, Chen Y, Cucurull L, Dymond KF, Ector D, et al. The COSMIC/FORMOSAT-3 mission-early results. Bulletin of the American Meteorological Society. 2008;**89**:313-333

[14] Anthes RA. Exploring Earth's atmosphere with radio occultation: Contributions to weather, climate and space weather. Atmospheric Measurement Techniques. 2011;**4**: 1077-1103. DOI: 10.5194/amt-4-1077-2011

[15] Kuo Y-H, Wee T-K, Sokolovskiy S, Rocken C, Schreiner W, Hunt D, et al. Inversion and error estimation of GPS radio occultation data. Journal of the

Meteorological Society of Japan. 2004;**82**:507-531

[16] Foelsche U, Pirscher B, Borsche M, Kirchengast G, Wickert J. Assessing the climate monitoring utility of radio occultation data: From CHAMP to FORMOSAT-3/COSMIC. Terrestrial, Atmospheric and Oceanic Sciences. 2009;**20**:155-170

[17] Ho S-P, Kirchengast G, Leroy S, Wickert J, Mannucci AJ, Steiner AK, et al. Estimating the uncertainty of using GPS radio occultation data for climate monitoring: Inter-comparison of CHAMP refractivity climate records 2002–2006 from different data centers. Journal of Geophysical Research. 2009;**114**:D23107. DOI: 10.1029/2009JD011969

[18] Ho S-P, Goldberg M, Kuo Y-H, Zou C-Z, Schreiner W. Calibration of temperature in the lower stratosphere from microwave measurements using COSMIC radio occultation data: Preliminary results. Terrestrial, Atmospheric and Oceanic Sciences. 2009;**20**: 87-100. DOI: 10.3319/TAO.2007.12.06. 01(F3C)

[19] Ho S-P, He W, Kuo Y-H. Construction of consistent temperature records in the lower stratosphere using global positioning system radio occultation data and microwave sounding measurements. In: Steiner AK et al., editors. New Horizons in Occultation Research. Berlin: Springer; 2009. pp. 207-217. DOI: 10.1007/978-3-642-00321-9_17

[20] Ho S-P, Kuo Y-H, Schreiner W, Zhou X. Using SI-traceable global positioning system radio occultation measurements for climate monitoring [in "States of the Climate in 2009"]. Bulletin of the American Meteorological Society. 2010;**91**(7):S36-S37

[21] Ho S-P, Zhou X, Kuo Y-H, Hunt D, Wang J-H. Global evaluation of radiosonde water vapor systematic biases using GPS radio occultation from COSMIC and ECMWF analysis. Remote Sensing. 2010;**2**(5):1320-1330

[22] Ho S-P, Hunt D, Steiner AK, Mannucci AJ, Kirchengast G, Gleisner H, et al. Reproducibility of GPS radio occultation data for climate monitoring: Profile-to-profile inter-comparison of CHAMP climate records 2002 to 2008 from six data centers. Journal of Geophysical Research. 2012;**117**:D18111. DOI: 10.1029/2012JD017665

[23] Kursinski ER, Hajj GA, Schofield JT, Linfield RP. Observing Earth's atmosphere with radio occultation measurements using the global positioning system. Journal of Geophysical Research. 1997;**102**(D19): 23429-23465

[24] Rocken C et al. Analysis and validation of GPS/MET data in the neutral atmosphere. Journal of Geophysical Research. 1997;**102**(D25): 29849-29866

[25] Kuo Y-H, Schreiner WS, Wang J, Rossiter DL, Zhang Y. Comparison of GPS radio occultation soundings with radiosondes. Geophysical Research Letters. 2005;**32**:L05817. DOI: 10.1029/ 2004GL021443

[26] He W, Ho S, Chen H, Zhou X, Hunt D, Kuo Y. Assessment of radiosonde temperature measurements in the upper troposphere and lower stratosphere using COSMIC radio occultation data. Geophysical Research Letters. 2009;**36**:L17807. DOI: 10.1029/ 2009GL038712

[27] Ho S-P, Peng L, Mears C, Anthes R. Comparison of global observations and trends of total precipitable water derived from microwave radiometers and COSMIC radio occultation from 2006 to 2013. Atmospheric Chemistry and Physics. 2018;**18**:259-274. https:// doi.org/10.5194/acp-18-259-2018

[28] Ho S-P, Peng L, Voemel H. Characterization of the long-term radiosonde temperature biases in the upper troposphere and lower stratosphere using COSMIC and Metop-A/GRAS data from 2006 to 2014. Atmospheric Chemistry and Physics. 2017;**17**:4493-4511. DOI: 10.5194/acp-17-4493-2017

[29] Hajj GA, Ao CO, Iijima BA, Kuang D, Kursinski ER, Mannucci AJ, et al. CHAMP and SAC-C atmospheric occultation results and inter-comparisons. Journal of Geophysical Research. 2004;**109**:D06109. DOI: 10.1029/2003JD003909

[30] Ho S-P, Kuo YH, Zeng Z, Peterson T. A comparison of lower stratosphere temperature from microwave measurements with CHAMP GPS RO data. Geophysical Research Letters. 2007;**34**:L15701. DOI: 10.1029/2007GL030202

[31] Trenberth KE, Guillemot CJ. Evaluation of the atmospheric moisture and hydrological cycle in the NCEP/NCAR reanalyses. Climate Dynamics. 1998;**14**:213-231

[32] Trenberth KE, Fasullo J, Smith L. Trends and variability in column integrated atmospheric water vapor. Climate Dynamics. 2005;**24**:741-758

[33] Sokolovskiy S, Kuo Y-H, Rocken C, Schreiner WS, Hunt D, Anthes RA. Monitoring the atmospheric boundary layer by GPS radio occultation signals recorded in the open-loop mode. Geophysical Research Letters. 2007;**33**:L12813. DOI: 10.1029/2006GL025955

[34] Ho S-P, Kuo YH, Sokolovskiy S. Improvement of the temperature and moisture retrievals in the lower troposphere using AIRS and GPS radio occultation measurements. Journal of Atmospheric and Oceanic Technology. 2007;**24**:1726-1173. DOI: 0.1175/JTECH2071.1

[35] Wang J, Zhang LY, Dai A, Van Hove T, Van Baelen J. A near-global, 2-hourly data set of atmospheric precipitable water vapor from ground-based GPS measurements. Journal of Geophysical Research. 2007;**112**:D11107

[36] Biondi R, Randel W, Ho S-P, Neubert T, Syndergaard S. Thermal structure of intense convective clouds derived from GPS radio occultations. Atmospheric Chemistry and Physics. 2012;**12**:5309-5318. DOI: 10.5194/acp-12-5309-2012

[37] Biondi R, Ho S-P, Randel W, Neubert T, Syndergaard S. Tropical cyclone cloud-top heights and vertical temperature structure detection using GPS radio occultation measurements. Journal of Geophysical Research. 2013;**118**:1-13. DOI: 10.1002/jgrd.50448

[38] Teng W-H, Huang C-Y, Ho S-P, Kuo Y-H, Zhou X-J. Characteristics of global precipitable water in ENSO events revealed by COSMIC measurements. Journal of Geophysical Research. 2013;**118**:1-15. DOI: 10.1002/jgrd.50371

[39] Scherllin-Pirscher B, Deser C, Ho S-P, Chou C, Randel W, Kuo Y-W. The vertical and spatial structure of ENSO in the upper troposphere and lower stratosphere from GPS radio occultation measurements. Geophysical Research Letters. 2012;**39**:L20801. DOI: 10.1029/2012GL053071

[40] Huang C-Y, Teng W-H, Ho S-P, Kuo Y-H. Global variation of COSMIC precipitable water over land: Comparisons with ground-based GPS measurements and NCEP reanalyses. Geophysical Research Letters. 2013;**40**:5327-5331. DOI: 10.1002/grl.50885

[41] Zeng Z, Ho S-P, Sokolovskiy S. The structure and evolution of Madden-Julian oscillation from FORMOSAT-3/COSMIC radio occultation data. Journal of Geophysical Research. 2012;**117**:D22108. DOI: 10.1029/2012JD017685

[42] Ma Z, Kuo Y-H, Ralph FM, Neiman PJ, Wick GA, Sukovich E, et al. Assimilation of GPS radio occultation data for an intense atmospheric river with the NCEP regional GSI system. Monthly Weather Review. 2011;**139**: 2170-2183. DOI: 10.1175/ 2011MWR3342.1

[43] Neiman PJ, Ralph FM, Wick GA, Kuo Y-H, Wee T-K, Ma Z, et al. Diagnosis of an intense atmospheric river impacting the Pacific Northwest: Storm summary and offshore vertical structure observed with COSMIC satellite retrievals. Monthly Weather Review. 2008;**136**:4398-4420

[44] Mears C, Wang J, Ho S-P, Zhang L, Zhou X. Global climate hydrological cycle, total column water vapor [in "State of the Climate in 2011"]. Bulletin of the American Meteorological Society. 2012;**93**(7):S25-S26. DOI: 10.1175

[45] Mears C, Wang J, Smith D, Wentz FJ. Intercomparison of total precipitable water measurements made by satellite-borne microwave radiometers and ground-based GPS instruments. Journal of Geophysical Research – Atmospheres. 2015;**120**:2492-2504. DOI: 10.1002/ 2014JD022694

[46] Mears C, Ho S-P, Peng L, Wang J. Total column water vapor, [in "State of the Climate in 2016"]. Bulletin of the American Meteorological Society. 2017; **98**(8):S93-S98. DOI: 10.1175/ 2017BAMSStateoftheClimate.1

[47] Strow LL, Hannon SE, DeSouza-Mackado S, et al. An overview of the AIRS radiative transfer model. IEEE Transactions on Geoscience and Remote Sensing. 2003;**41**(2):303-313

[48] Liu C-Y, Li J, Ho S-P, Liu G-R, Lin T-H, Young C-C. Retrieval of atmospheric thermodynamic state from synergistic use of radio occultation and hyperspectral infrared radiances observations. IEEE Journal of Selected Topics in Applied Earth Observations and Remote Sensing. 2016;**9**:744-756. DOI: 10.1109/JSTARS.2015.2444274

[49] Wick GA, Kuo Y-H, Ralph FM, Wee T-K, Neiman PJ, Ma Z. Intercomparison of integrated water vapor retrievals from SSM/I and COSMIC. Geophysical Research Letters. 2008;**28**:3263-3266